in putting the discussion of bonding in this type of complex on a more quantitative basis.

Experimental Section

UV-visible spectra were recorded with a Varian-Cary 118 C spectrophotometer. The energy of the MLCT transition was determined from the spectrum of a freshly prepared aqueous solution of each complex at room temperature. The pyrimidine and pyridazine complexes of pentacyanoferrate(II) were prepared in solution according to the procedure described by Toma and Malin for other complexes of the series.[2a] The pentacyanoruthenate(II) complexes were prepared by allowing an excess of the ligand, L, to react with a solution of $(CN)_5RuOH_2^{3-}$. Solutions of $(CN)_5RuOH_2^{3-}$ were prepared from the reaction of Br_2 with $Ru(CN)_6^{4-}$.[18] Details of the synthetic procedure are given elsewhere.[14] With the exception of *N*-methylpyrazinium ion, the ligand was added to the solution of $Ru(CN)_6^{4-}$ prior to adding Br_2. In the *N*-methylpyrazinium case, the ligand was added immediately after the Br_2. The solid complexes were isolated by precipitation with cold acetone for L = pyridine, 4-methylpyridine, 4,4′-bipyridine, pyrimidine, pyridazine, pyrazine, 2-methylpyrazine, isonicotinamide, isonicotinic acid, and *N*-methylpyrazinium ion. The spectra of complexes with other ligands were obtained on the reaction mixture or after isolation of the complex on an anion-exchange resin and elution with 4 M $NaClO_4$. The spectra of the redissolved solids were in agreement with spectra of the reaction mixture prior to isolation of the complex. The isolated solids were characterized by NMR.[19] Over the time of 1 day, solutions of the pentacyanoruthenate(II) complexes undergo slow spectral changes, indicating some aquation or decomposition.

Acknowledgment. The authors are grateful for support of this work through National Science Foundation Grant No. CHE 802 183.

Registry No. $(CN)_5FeL^{3-}$ (L = pyrimidine), 86260-12-0; $(CN)_5FeL^{3-}$ (L = pyridazine), 86260-13-1; $(CN)_5RuL^{3-}$ (L = 4-methylpyridine), 86260-14-2; $(CN)_5RuL^{3-}$ (L = pyridine), 86260-15-3; $(CN)_5RuL^{3-}$ (L = pyrimidine), 86260-16-4; $(CN)_5RuL^{4-}$ (L = isonicotinato), 86260-17-5; $(CN)_5RuL^{3-}$ (L = isonicotinic acid), 86260-18-6; $(CN)_5RuL^{3-}$ (L = pyridazine), 86260-19-7; $(CN)_5RuL^{3-}$ (L = 2-methylpyrazine), 86260-20-0; $(CN)_5RuL^{3-}$ (L = isonicotinamide), 86260-21-1; $(CN)_5RuL^{3-}$ (L = 4,4′-bipyridine), 86260-22-2; $(CN)_5RuL^{3-}$ (L = 4-cyanopyridine), 86260-23-3; $(CN)_5RuL^{3-}$ (L = 4-formylpyridine), 86260-24-4; $(CN)_5RuL^{2-}$ (L = *N*-methylpyrazinium), 84711-78-4.

Contribution from the Department of Chemistry, The University of North Carolina, Chapel Hill, North Carolina 27514

Photochemistry of MLCT Excited States. Effect of Nonchromophoric Ligand Variations on Photophysical Properties in the Series *cis*-$Ru(bpy)_2L_2^{2+}$

JONATHAN V. CASPAR and THOMAS J. MEYER*

Received September 10, 1982

The photophysical properties of the low-lying, emissive metal to ligand charge transfer (MLCT) excited states of a series of complexes of the type *cis*-$Ru(bpy)_2L_2^{2+}$ (L = pyridine, pyridazine, $^1/_2$ phenanthroline, $^1/_2$ bipyridine, *N*-methylimidazole, 2-(2-aminoethyl)pyridine) have been investigated. The results lead to a self-consistent picture of the roles of different decay pathways in determining excited-state lifetimes. The lifetime of the MLCT excited state(s) is shown to be dictated by (1) a radiative decay pathway (k_r) that is relatively insensitive to variations in L, (2) a nonradiative transition to the ground state (k_{nr}), the rate constant for which varies as predicted by the energy gap law for radiationless transitions, and (3) the rate of a thermally activated transition between the MLCT state and a low-lying, metal-centered dd excited state. It is the latter transition and the role that the ligands L play in stabilizing the MLCT state relative to the dd state that provide a reasonable explanation for the absence of room-temperature emission and/or the appearance of ligand-loss photochemistry in cases where L is a phosphine, arsine, or CO group.

The low-lying metal to ligand charge transfer (MLCT) excited state(s) of the ion $Ru(bpy)_3^{2+}$ (bpy is 2,2′-bipyridine) has been used in a number of photosensitization schemes.[1] The bases for its popularity include the following: (1) The ion is easily prepared and relatively stable toward photodecomposition. (2) The MLCT excited state(s) is long-lived at room temperature in fluid solution. (3) The excited state luminesces visibly at room temperature in fluid solution, which provides a valuable spectral probe for monitoring photochemical processes. (4) The excited state undergoes facile energy transfer or electron transfer, in the latter case to give stable oxidized, $Ru(bpy)_3^{3+}$, or reduced, $Ru(bpy)_3^{+}$, products.

In order to design new and perhaps more elaborate sensitizers related to $Ru(bpy)_3^{2+}$, it is important to understand the factors that are important in dictating its excited-state properties. In fact, the results of a variety of experimental and theoretical studies have led to an increasingly detailed account of the excited-state structure of $Ru(bpy)_3^{2+}$:

(1) The absorption spectrum is dominated by optical transitions to MLCT states largely singlet in character.[2]

(2) Following optical excitation, rapid ($\tau < 1$ ps), efficient ($\phi \sim 1$) decay occurs to the emitting MLCT state(s), which are largely triplet in character.[3] The effect of spin-orbit coupling is to mix the singlet and triplet states, but the two different types of states retain much of their initial spin character.

(3) The emitting, redox-active state is really a manifold of three closely spaced states largely triplet in character. A fourth slightly higher state may also exist, having a greater degree of singlet character than the lower three.[4,6e]

(4) In the low-lying MLCT states, the excited electron appears to be localized on a single ligand although no doubt transferring between ligands on a relatively short time scale.[5]

(1) (a) Balzani, V.; Bolleta, F.; Gandolfi, M. T.; Maestri, M. *Top. Curr. Chem.* **1978**, *75*, 1. (b) Sutin, N.; Creutz, C. *Pure Appl. Chem.* **1980**, *52*, 2717. (c) Sutin, N. *J. Photochem.* **1979**, *10*, 19. (d) Kalyanasundaram, K. *Coord. Chem. Rev.* **1982**, *46*, 159.

(2) (a) Felix, F.; Ferguson, J.; Gudel, H. U.; Ludi, A. *J. Am. Chem. Soc.* **1980**, *102*, 4096. (b) Kober, E. M.; Meyer, T. J. *Inorg. Chem.* **1982**, *21*, 3967.

(3) (a) Creutz, C.; Chan, M.; Netzel, T. L.; Okumura, M.; Sutin, N. *J. Am. Chem. Soc.* **1980**, *102*, 1309. (b) Demas, J. N.; Taylor, D. G. *Inorg. Chem.* **1979**, *18*, 3177. (c) Hager, G. D.; Crosby, G. A. *J. Am. Chem. Soc.* **1975**, *97*, 7031. (d) Hipps, K. W.; Crosby, G. A. *Ibid.* **1975**, *97*, 7042. (e) Hager, G. D.; Watts, R. J.; Crosby, G. A. *Ibid.* **1975**, *97*, 7037. (f) Crosby, G. A. *Acc. Chem. Res.* **1975**, *8*, 231.

(4) Kober, E. M.; Meyer, T. J., manuscript in preparation. Yersin, H. private communication.

(5) Bradley, P. G.; Kress, N.; Hornberger, B. A.; Dallinger, R. F.; Woodruff, W. H. *J. Am. Chem. Soc.* **1981**, *103*, 7441.

0020-1669/83/1322-2444$01.50/0

(5) Photochemical and photophysical studies on $Ru(bpy)_3^{2+}$ show that, in addition to the manifold of MLCT states, a low-lying Ru-localized dd excited state exists, which is populated by thermal activation from the low-lying, triplet states.[6]

(6) The dd state accounts for the observed photosubstitutional chemistry of $Ru(bpy)_3^{2+}$ and represents a major deactivation pathway for the MLCT state at room temperature.[6a,7]

A general kinetic scheme that has proven useful in explaining the observed excited-state dynamic behavior of $Ru(bpy)_3^{2+}$ is shown in Scheme I. ^{1}MLCT represents the manifold of states largely singlet in character that dominate light absorption, and ^{3}MLCT is the manifold of states largely triplet in character that are involved in emission.

Scheme I

$$\text{ground state} \xrightarrow{h\nu} {}^1\text{MLCT}$$

$${}^1\text{MLCT} \xrightarrow{\phi_{isc} \sim 1} {}^3\text{MLCT}$$

$${}^3\text{MLCT} \xrightarrow{k_r} \text{ground state} + h\nu' \text{ (emission)}$$

$${}^3\text{MLCT} \xrightarrow{k_{nr}} \text{ground state} + \text{heat (nonradiative decay)}$$

$${}^3\text{MLCT} \underset{k_{-2}}{\overset{k_2}{\rightleftharpoons}} \text{dd}$$

$$\text{dd} \xrightarrow{k_3} \text{ground state or photochemistry}$$

An important ingredient in any attempt to prepare new excited states based on Ru–polypyridyl chromophores is a detailed understanding of how chemical changes influence excited-state photophysical and photochemical properties. The properties of note include (1) excited-state lifetime, as determined by the rates of radiative (k_r) and nonradiative (k_{nr}) processes and by rates for the population and subsequent decay of low-lying dd states, (2) photochemical instability, which is dictated by the availability of low-lying dd states and by their inherent reactivity,[6a,b,7] and (3) ground-state and excited-state redox potentials.[8]

In this paper we address the question of how variations in nonchromophoric ligands affect both the MLCT ($d\pi^5\pi^*$) → ground state ($d\pi^6$) and MLCT ($d\pi^5\pi^*$) → dd ($d\pi^5 d\sigma^*$) transitions in a series of complexes of the type $Ru(bpy)_2L_2^{2+}$, where L is a N-donor ligand. The results are of significance for what they reveal about the effects of ligand variations on excited-state properties for the series. In addition, values for nonradiative decay rate constants are made available for comparisons with values obtained earlier for the closely related series of MLCT excited states $Os^{II}(bpy)L_4^{2+}$ and $Os^{II}(phen)L_4^{2+}$ (phen is 1,10-phenanthroline; L = CO, PR_3, AsR_3, $(bpy)_{1/2}$, $(phen)_{1/2}$, CH_3CN, etc.),[9] for a series of Re(I)–bpy MLCT excited states of the type $Re^I(bpy)(CO_3L^+$ (L = substituted pyridines, CH_3CN, PR_3),[10] and for the effect of solvent on nonradiative decay in $Ru(bpy)_3^{2+}$.[6b]

Chart I

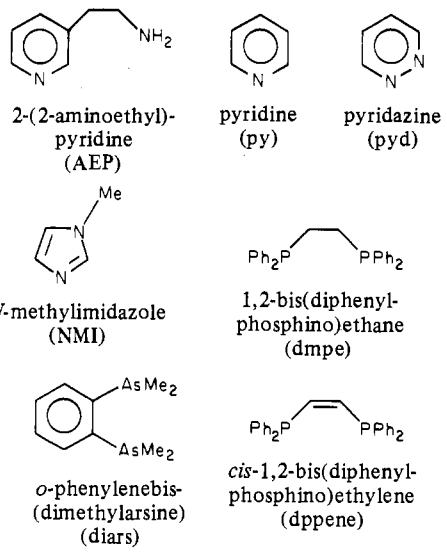

Experimental Section

Materials. The complexes $[Ru(bpy)_3](PF_6)_2$,[11a] $[Ru(bpy)_2(AEP)](PF_6)_2$[12] (AEP = 2-(2-aminoethyl)pyridine), $[Ru(bpy)_2(pyd)_2](PF_6)_2$ (pyd = pyridazine), $[Ru(bpy)_2(py)_2](PF_6)_2$[13] (py = pyridine), $[Ru(bpy)_2(phen)](PF_6)_2$,[11b] and $[Ru(bpy)_2(NMI)_2](PF_6)_2$ (NMI = *N*-methylimidazole) were prepared by literature methods from *cis*-$Ru(bpy)_2Cl_2$[14] and an excess of ligand heated at reflux in 1:1 EtOH/water for approximately 3 h. The complexes $[Ru(bpy)_2(P)_2](PF_6)_2$ (P = monodentate phosphine or $^1/_2$ chelate phosphine) were prepared as described previously.[14] $[Ru(bpy)_2(CO)Cl](PF_6)$ was obtained by the reaction of $[Ru(bpy)_2Cl_2]$ and CO at reflux in 2-methoxyethanol for 1.5 h, followed by precipitation of the product with excess NH_4PF_6.[15] The complexes were purified by column chromatography on alumina with acetonitrile/toluene mixtures as eluants. The complexes $Ru(bpy)_2L_2^{2+}$ (L = py, pyd) and $Ru(bpy)_2(CO)Cl^+$ are extremely labile photochemically in solution and were purified in the dark.[16] Satisfactory elemental analyses were obtained for all complexes. Cyclic voltammetry measurements were carried out in CH_3CN solution at a platinum-bead electrode with 0.1 M $(NEt_4)ClO_4$ as supporting electrolyte with an apparatus described previously.[17]

All solvents were of reagent grade and were used as received. For lifetime, emission, and electrochemical studies, high-purity methylene chloride and acetonitrile were obtained from Burdick-Jackson Laboratories and used without further purification.

Emission Studies. Emission spectra were obtained on an SLM 8000 photon-counting spectrofluorimeter and were corrected for detector sensitivity with use of data and programs supplied by the manufacturer. Measurements of emission spectra at 200 K were carried out with an Oxford Instruments liquid-nitrogen cryostat. Emission quantum yields in methylene chloride solution at 25 °C were determined in deoxygenated solution (Ar bubbling for 20 min) with an aqueous solution of $[Ru(bpy)_3](PF_6)_2$ as a standard (ϕ_r = 0.042),[6d] and corrections were made for the differences in the refractive indices of the two solvents.[18]

(6) (a) Durham, B.; Caspar, J. V.; Nagle, J. K.; Meyer, T. J. *J. Am. Chem. Soc.* **1982**, *104*, 4803. (b) Caspar, J. V.; Meyer, T. J. *J. Am. Chem. Soc.*, in press. (c) Allsop, S. R.; Cox, A.; Kemp, T. J.; Reed, W. J. *J. Chem. Soc., Faraday Trans. 1* **1977**, *73*, 1275. (d) Van Houten, J.; Watts, R. J. *J. Am. Chem. Soc.* **1976**, *98*, 4853. (e) Allsop, S. R.; Cox, A.; Jenkins, S. H.; Kemp, T. J.; Tunstall, S. M. *Chem. Phys. Lett.* **1976**, *43*, 135.
(7) (a) Van Houten, J.; Watts, R. J. *Inorg. Chem.* **1978**, *17*, 3381. (b) Wallace, W. M.; Hoggard, P. E. *Ibid.* **1980**, *19*, 2141. (c) Porter, G. B.; Sparks, R. H. *J. Photochem.* **1980**, *13*, 123.
(8) Bock, C. R.; Connor, J. A.; Gutierrez, A. R.; Meyer, T. J.; Whitten, D. G.; Sullivan, B. P.; Nagle, J. K. *J. Am. Chem. Soc.* **1979**, *101*, 4815.
(9) (a) Kober, E. M.; Sullivan, B. P.; Dressick, W. J.; Caspar, J. V.; Meyer, T. J. *J. Am. Chem. Soc.* **1980**, *102*, 7383. (b) Caspar, J. V.; Kober, E. M.; Sullivan, B. P.; Meyer, T. J. *Ibid.* **1982**, *104*, 630.
(10) Caspar, J. V.; Meyer, T. J. *J. Phys. Chem.* **1983**, *87*, 952.
(11) (a) Braddock, J. N.; Meyer, T. J. *J. Am. Chem. Soc.* **1973**, *95*, 3158. (b) Crosby, G. A.; Elfring, W. H., Jr. *J. Phys. Chem.* **1976**, *80*, 2206.
(12) Brown, G. M.; Weaver, T. R.; Keene, R. F.; Meyer, T. J. *Inorg. Chem.* **1976**, *15*, 190.
(13) Dwyer, F. P.; Goodwin, H. A.; Gyarfas, E. C. *Aust. J. Chem.* **1963**, *16*, 544.
(14) Sullivan, B. P.; Salmon, D. J.; Meyer, T. J. *Inorg. Chem.* **1978**, *17*, 3334.
(15) (a) Sullivan, B. P.; Caspar, J. V.; Meyer, T. J., manuscript in preparation. (b) Clear, J. M.; Kelly, J. M.; O'Connel, C. M.; Vos, J. G.; Cardin, C. J.; Costa, C. R.; Edwards, A. J. *J. Chem. Soc., Chem. Commun.* **1980**, 750.
(16) Durham, B.; Walsh, J. L.; Carter, C. L.; Meyer, T. J. *Inorg. Chem.* **1980**, *19*, 860.
(17) Calvert, J. M.; Meyer, T. J. *Inorg. Chem.* **1981**, *20*, 27.
(18) (a) Demas, J. N.; Crosby, G. A. *J. Phys. Chem.* **1971**, *75*, 991. (b) Ediger, M. D.; Mog, R. S.; Boxer, S. G.; Fayer, M. D. *Chem. Phys. Lett.* **1982**, *88*, 123.

Table I. Luminescence Data

compd	$10^{-3}E_{em}(0\text{-}0)$,[a] cm^{-1}	$\bar{\nu}_M$,[a] cm^{-1}	ϕ_r[b]	$10^{-3}E_{em}$(200 K),[c] cm^{-1}	$10^{-3}E'_{em}(0\text{-}0)$,[d] cm^{-1}	$10^{-3}E_{em}$(298 K),[e] cm^{-1}
$Ru(bpy)_2(AEP)^{2+}$	15.70	1310	6.6×10^{-3}	15.31	15.39	15.50
$Ru(bpy)_2(NMI)_2^{2+}$	15.80	1330	3.4×10^{-2}	14.53	14.65	14.66
$Ru(bpy)_2(py)_2^{2+}$	16.98	1330	4.2×10^{-3}	16.53	16.66	16.42
$Ru(bpy)_3^{2+}$	17.12	1350	2.9×10^{-2}	16.58	16.66	16.50
$Ru(bpy)_2(phen)^{2+}$	17.24	1340	3.3×10^{-2}	16.69	16.73	16.64
$Ru(bpy)_2(pyd)_2^{2+}$	17.42	1370	2.7×10^{-4}	16.86	16.96	16.39
$Ru(bpy)_2(dmpe)^{2+}$	17.95	[f]				
$Ru(bpy)_2(diars)^{2+}$	18.15	1450				
trans-$Ru(bpy)_2(PPh_2Me)_2^{2+}$	18.21	~1200[f]				
cis-$Ru(bpy)_2(PPh_2Me)_2^{2+}$	18.52	~1100[f]				
$Ru(bpy)_2(dppene)^{2+}$	19.30	~1100[f]				
$Ru(phen)_3^{2+}$			1.00×10^{-2}	17.12		17.01

[a] The 0-0 emission energy and vibrational spacing ($\bar{\nu}_M$) in 4:1 EtOH/MeOH glass at 77 K. [b] Radiative efficiencies determined at 298 K in deoxygenated CH_2Cl_2 solution. [c] CH_2Cl_2 solution at 200 K. [d] From spectral fits of the emission spectrum at 200 K in methylene chloride solution. [e] CH_2Cl_2 solution at 298 K. [f] Vibrational structure poorly resolved.

Lifetimes. Variable-temperature emission lifetimes (τ_0) were determined by laser flash photolysis in deoxygenated methylene chloride solution (Ar bubble, 20 min) with an apparatus described previously.[19] The temperature-dependent lifetimes were fit to the expression

$$\frac{1}{\tau_0(T)} = k + k^{\circ} \exp(-\Delta E'/k_B T) \quad (1)$$

where $k = k_r + k_{nr}$ and k_r and k_{nr} are respectively the radiative and nonradiative decay rate constants for the MLCT excited states. All lifetime data were acquired at temperatures above the freezing point of methylene chloride. Values for k_r and k_{nr} were obtained by using eq 2 and 3, where ϕ_r is the emission quantum yield at 25 °C. When

$$k_r = \phi_r/\tau_0(25\ ^{\circ}C) \quad (2)$$

$$k_{nr} = k - k_r \quad (3)$$

eq 1 is used, it is assumed that k_r and k_{nr} are only weakly temperature dependent in the region of interest. Studies on $Ru(bpy)_3^{2+}$ have shown this approximation to be valid.[6] The lifetime measurements were carried out by excitation into higher MLCT states largely singlet in character,[2] and as a result, ϕ_r in eq 2 is really the product of an intersystem crossing efficiency, ϕ_{isc}, and the true radiative efficiency, ϕ'_r. If $\phi_{isc} \neq 1$, $k_r = \phi_r/(\tau_0\phi_{isc})$, but such a correction would have virtually no effect on the conclusions reached here because the radiative efficiencies are low (Table I) and $1/\tau_0 \sim k_{nr} + k^{\circ} \exp(-\Delta E'/k_B T)$. It is known for $Ru(bpy)_3^{2+}$ that $\phi_{isc} \sim 1.0$ in fluid solution at room temperature.[3b]

Results

Structures, names, and abbreviations for the ligands, L, used in this study are shown in Chart I.

Emission Spectra. The emission spectra of the $Ru(bpy)_2L_2^{2+}$ complexes at 77 K in 4:1 EtOH/MeOH glasses (Figure 1) are all characterized by a well-defined vibrational progression with the spacings ($\bar{\nu}_M$) between the first two components ranging from 1310 to 1370 cm^{-1}. Emission spectra of this type are typical for MLCT excited states with bipyridine as the chromophoric ligand. The vibrational progressions appear to be assignable to a ν(bpy) framework vibration(s).[3f,5,9] Values of the $v'_M = 0 \rightarrow v_M = 0$ emission energies ($E_{em}(0\text{-}0)$) and of the vibrational frequencies as $\bar{\nu}_M$ ($=1/\lambda_M$) obtained from the spacings between components are given in Table I. Also included in Table I are values of the radiative quantum yield (ϕ_r) at 298 K and of the emission energy at the intensity maximum (E_{em}) in methylene chloride solution at 200 and 298 K. With the exception of $Ru(bpy)_2(NMI)^{2+}$, at 200 K all of the complexes show a broad emission manifold with a pronounced shoulder on the low-energy side (Figure 2) corresponding to the $v'_M = 0 \rightarrow v_M = 1$ vibrational component, which is clearly observed at 77 K in alcohol glasses. The increase in the half-width of the vibrational components with increasing temperature produces the poorly resolved high-temperature spectra. At 298 K, all of the complexes show broad structureless emissions that tail to lower energy (Figure 3). Gaussian decomposition of the vibrational components of the observed 200 K emission spectra can be used to obtain values of the vibrational spacing as $\bar{\nu}_M$, the excited-state distortion (S_M), the $v'_M = 0 \rightarrow v_M = 0$ emission energy ($E_{em}(0\text{-}0)$), and the full-width at half-maximum of the individual

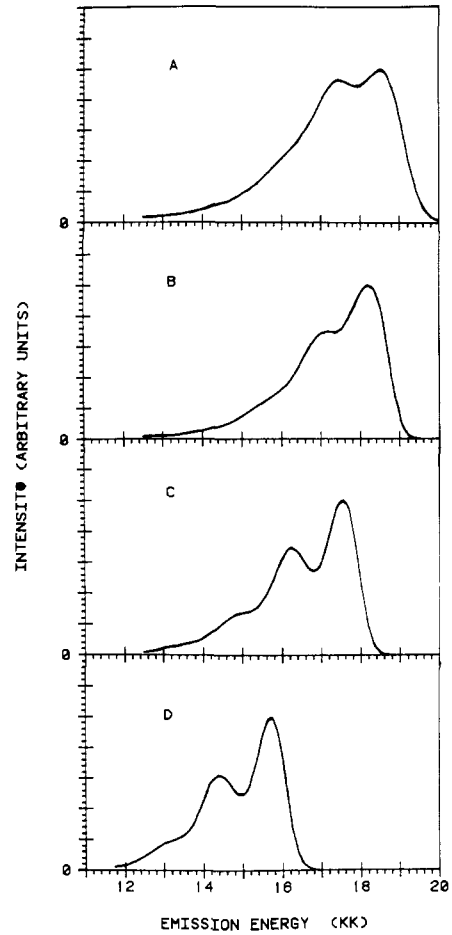

Figure 1. Typical emission spectra for complexes of the type $Ru(bpy)_2L_2^{2+}$ at 77 K in 4:1 methanol/ethanol glass (spectra corrected for detector sensitivity): A, *cis*-$[Ru(bpy)_2(PPh_2Me)_2](PF_6)_2$; B, *trans*-$[Ru(bpy)_2(PPh_2Me)_2](PF_6)_2$; C, *cis*-$[Ru(bpy)_2(pyd)_2](PF_6)_2$; D, $[Ru(bpy)_2(AEP)](PF_6)_2$.

(19) Nagle, J. K. Ph.D. Dissertation, The University of North Carolina, Chapel Hill, NC, 1979.
(20) Herzberg, G. "Molecular Spectra and Molecular Structure"; Van Nostrand: New York, 1950; Vol. 1, Chapter 4.

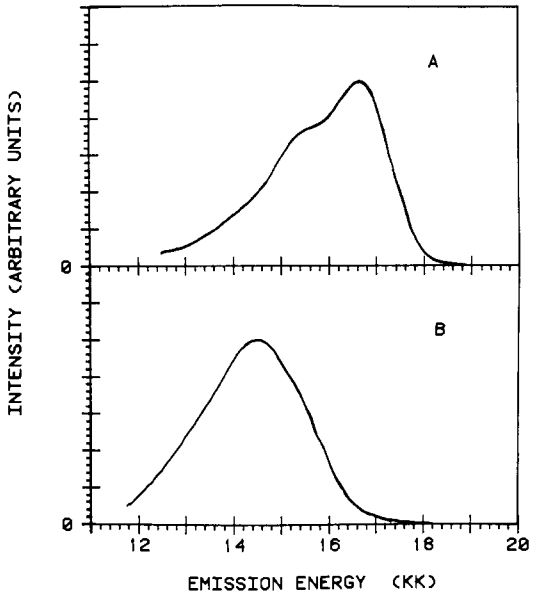

Figure 2. Typical emission spectra for *cis*-$Ru(bpy)_2L_2^{2+}$ complexes at 200 K in methylene chloride solution (spectra corrected for detector sensitivity); A, $[Ru(bpy)_2(phen)](PF_6)_2$; B, $[Ru(bpy)_2(NMI)_2](PF_6)_2$.

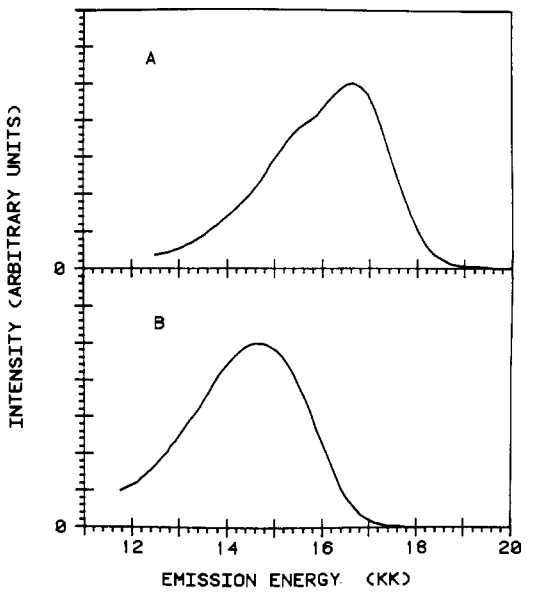

Figure 3. Typical emission spectra for complexes of the type *cis*-$Ru(bpy)_2(L)_2^{2+}$ at 298 K in methylene chloride solution: A, $[Ru(bpy)_2(phen)](PF_6)_2$; B, $[Ru(bpy)_2(NMI)_2](PF_6)_2$.

vibrational components ($\bar{\nu}_{1/2}$). The expression for the band shape is given in eq 4, where $I(E)$ is the emission intensity at

$$I(E) = \sum_{v=0}^{N}\left(\frac{E_{em}(0\text{–}0) - v\hbar\omega_M}{E_{em}(0\text{–}0)}\right)^4\left(\frac{S_M^v}{v!}\right) \exp\left[-4\log\left(2\left(\frac{E - E_{em}(0\text{–}0) + v\hbar\omega_M}{\bar{\nu}_{1/2}}\right)^2\right)\right] \quad (4)$$

energy E. S_M will be defined later and the term $\hbar\omega_M = h\nu_M$, which appears in eq 4, is related to $\bar{\nu}_M$ by $\bar{\nu}_M = \omega_M/2\pi c = \nu_M/c$, where c is the speed of light in a vacuum. From the values of $\bar{\nu}_M$ obtained at 77 K, S_M values in the range of 0.7–1.0, and $\bar{\nu}_{1/2}$ = 1200–1600 cm^{-1}, the values of $E_{em}(0\text{–}0)$ at 200 K were obtained by an iterative fitting procedure to the experimental spectra. A typical fit is shown in Figure 4 for $Ru(bpy)_3^{2+}$ in CH_2Cl_2 solution at 200 K, using values of $\bar{\nu}_M$ = 1350 cm^{-1}, S_M = 0.96, $\bar{\nu}_{1/2}$ = 1400 cm^{-1}, and $E_{em}(0\text{–}0)$ = 16 660 cm^{-1}. Values of $E_{em}(0\text{–}0)$ at 200 K in methylene chloride solution for all of the complexes are presented in Table I. Note that E_{em} at 200 K is on the average approximately only 90 cm^{-1} lower in energy than $E_{em}(0\text{–}0)$. This is a consequence of the fact that values of S_M and of $\bar{\nu}_{1/2}/\bar{\nu}_M$ (~1.1) are small for these complexes.

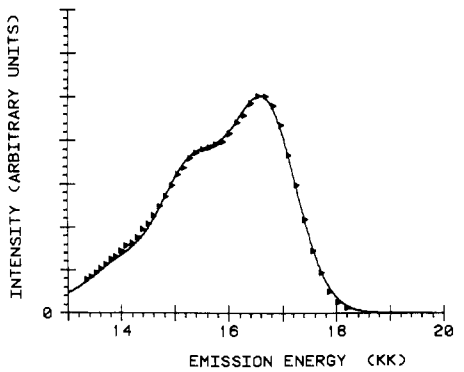

Figure 4. Emission spectrum of $[Ru(bpy)_3](PF_6)_2$ at 200 K in methylene chloride solution (▲) and the theoretical fit using the expression in eq 4 with $\hbar\omega_M$ = 1350 cm^{-1}, S_M = 0.96, $\bar{\nu}_{1/2}$ = 1400 cm^{-1}, and $E_{em}(0\text{–}0)$ = 16 660 cm^{-1}.

It should be noted that, in fitting the observed emission spectra to eq 4, the approximation is made of a single high-frequency vibrational progression. We have in fact found that in order to fit the 77 K emission spectra of $Ru(bpy)_2L_2^{2+}$, $Os(bpy)L_4^{2+}$, and $Os(phen)L_4^{2+}$ complexes quantitatively, it is necessary to introduce contributions from a low-frequency (~400 cm^{-1}) vibration or vibrations. The low-frequency vibrations are no doubt associated with metal–ligand bond length changes in the excited state. Contributions from low-frequency vibrations appear to be least important for nitrogen-donor ligands and of increasing importance for ligands of the type PR_3, AsR_3, or Cl^-. These effects appear in the spectra in Figure 1 since as the distortion in the low-frequency vibration increases, the high-frequency vibrational progressions become less well resolved. Since all of the complexes of interest for the photophysical experiments described here contain only nitrogen-based ligands in the coordination sphere, the approximation involved in using eq 4 to fit the 200 K spectra should be adequate. The quantitative fit of the 77 K spectra to both high- and low-frequency vibrations will be the topic of a forthcoming publication.[21b]

Electrochemistry. Cyclic voltammetry for all of the complexes studied here shows one reversible Ru(II)/Ru(III) oxidation wave at positive potentials vs. the saturated sodium chloride calomel electrode (SSCE). At negative potentials the complexes show two reversible reductions assignable to the ligand-based couples $Ru(bpy)_2(L)_2^{2+}/Ru(bpy^-\cdot)(bpy)(L)_2^+$ and $Ru(bpy^-\cdot)(bpy)(L)_2^+/Ru(bpy^-\cdot)_2(L)_2$. $Ru(bpy)_3^{2+}$ shows a third reduction associated with the presence of the third bipyridine ligand. For the complex $[Ru(bpy)_2(phen)](PF_6)_2$ the ligand-based reductions are not reversible due to adsorption of the reduction products. Table II summarizes the electrochemical properties of a series of $Ru(bpy)_2L_2^{2+}$ complexes.

Emission Lifetimes. Temperature-dependent lifetimes were fit to the expression in eq 1.[6a] An example of a typical data set and the resulting theoretical fit are shown in Figure 5, where $\ln \tau_0(T)$ vs. $1/T$ is shown plotted for $[Ru(bpy)_2(phen)]^{2+}$ in methylene chloride solution. Values of the parameters k, k^∞, and $\Delta E'$ obtained from the fits are summarized in Table III. From the values of ϕ_r in Table I and eq 2 and 3, k can be partitioned into its components k_r and k_{nr}. Results of these

(21) (a) Yersin, H.; Otto, H.; Zink, J. I.; Gliemann, G. *J. Am. Chem. Soc.* **1980**, *102*, 951. (b) Caspar, J. V.; Meyer, T. J., manuscript in preparation. (c) Caspar, J. V. Ph.D. Dissertation, The University of North Carolina, Chapel Hill, NC, 1982.

Table II. Reduction Potentials for Excited- and Ground-State Redox Couples[a]

compd	$E_{1/2}(3+/2+)$	$E_{1/2}(bpy/bpy^{-}\cdot)$	$\Delta E_{1/2}$[b]	$E_{1/2}(3+/2+^{*})$[c]	$E_{1/2}(2+^{*}/+)$[d]
$Ru(bpy)_2(AEP)^{2+}$	1.02	−1.44	2.46	−0.93	0.51
$Ru(bpy)_2(NMI)_2^{2+}$	0.94	−1.48	2.42	−1.02	0.48
$Ru(bpy)_2(py)_2^{2+}$	1.25	−1.35	2.60	−0.86	0.76
$Ru(bpy)_3^{2+}$	1.22	−1.36	2.58	−0.90	0.76
$Ru(bpy)_2(phen)^{2+}$	1.23	~−1.36[e]	~2.59	−0.91	0.78
$Ru(bpy)_2(pyd)_2^{2+}$	1.24	−1.38	2.62	−0.92	0.78
$Ru(bpy)_2(CO)Cl^{2+}$	1.46	−1.30	2.76		
$Ru(bpy)_2(dmpe)^{2+}$	1.40	−1.38	2.78	−0.83	0.85
$Ru(bpy)_2(diars)^{2+}$	1.45	−1.36	2.81	−0.80	0.89
trans-$Ru(bpy)_2(PPh_2Me)_2^{2+}$	1.46	~−1.30[e]	~2.76	−0.80	0.96
cis-$Ru(bpy)_2(PPh_2Me)_2^{2+}$	1.55	−1.28	2.83	−0.75	1.02
$Ru(bpy)_2(dppene)^{2+}$	1.75	−1.28	3.03	−0.64	1.11

[a] Volts vs. SSCE in CH_3CN solution with 0.1 M tetraethylammonium perchlorate as supporting electrolyte. Potentials are not corrected for junction potential effects. The $E_{1/2}$ values are formal potentials except for a usually small term involving the ratio of diffusion coefficients. $E_{1/2}(3+/2+)$ refers to the metal-based Ru(III)/Ru(II) couple and $E_{1/2}(bpy)/(bpy^{-}\cdot)$ to the first ligand-based couple. [b] $\Delta E_{1/2} = E_{1/2}(Ru(III)/Ru(II)) - E_{1/2}(bpy/bpy^{-}\cdot)$ in volts. [c] Excited-state potentials for the couple $Ru(bpy)_2(L)_2^{3+}/Ru(bpy)_2(L)_2^{2+*}$ calculated from eq 5 by using the value of $E_{em}(0\text{-}0)$ measured at 77 K in 4:1 methanol/ethanol glass for E_{em}. [d] Excited-state potentials for the couple $Ru(bpy)_2(L)_2^{2+*}/Ru(bpy)_2(L)_2^{+}$ calculated from eq 6 by using the value of $E_{em}(0\text{-}0)$ measured at 77 K in 4:1 methanol/ethanol glass for E_{em}. [e] Adsorption obscures the return wave. $E_{1/2}(bpy/bpy^{-}\cdot)$ estimated as $E_{p,c} + 0.03$ eV.

Table III. Kinetic Parameters for the Decay of the MLCT Excited States of the Complexes $Ru(bpy)_2L_2^{2+}$ in CH_2Cl_2 Solution[a]

compd	τ_0(298 K), μs	k, s^{-1}	k'°, s^{-1}	$\Delta E'$, cm^{-1}	k_r, s^{-1}	k_{nr}, s^{-1}
$Ru(bpy)_2(NMI)_2^{2+}$	0.31	2.5×10^6	1.5×10^{13}	3500	1.10×10^5	2.4×10^6
$Ru(bpy)_2(AEP)^{2+}$	0.12[b]	9.1×10^5	4.5×10^{13}	3240	5.7×10^4	8.5×10^5
$Ru(bpy)_2(py)_2^{2+}$	0.47[b]	8.2×10^5	1.7×10^{13}	3410	8.9×10^3	8.1×10^5
$Ru(bpy)_3^{2+}$	0.49	4.1×10^5	4.5×10^{13}	3560	5.9×10^4	3.5×10^5
$Ru(bpy)_2(phen)^{2+}$	0.31[b]	3.7×10^5	6.9×10^{13}	3550	1.0×10^5	2.7×10^5
$Ru(bpy)_2(pyd)_2^{2+}$	0.31[b]	3.4×10^5	1.5×10^{14}	2710	9.3×10^4	2.5×10^5
$Ru(phen)_3^{2+}$	0.13[b]	1.4×10^5	3.1×10^{13}	3180	7.2×10^4	6.75×10^4

[a] The variables are defined in the text; note eq 1. [b] Calculated from the temperature-dependent data by using eq 1.

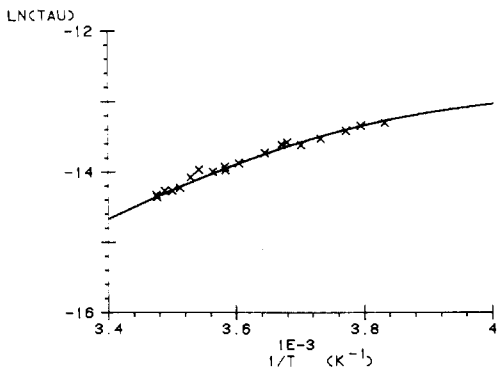

Figure 5. Plot of ln τ_0 vs. $1/T$ (K^{-1}) for the MLCT decay of $[Ru(bpy)_2(phen)](PF_6)_2$ in methylene chloride solution. The solid line is the fit calculated by using the expression in eq 1, and the values of the parameters are shown in Table III.

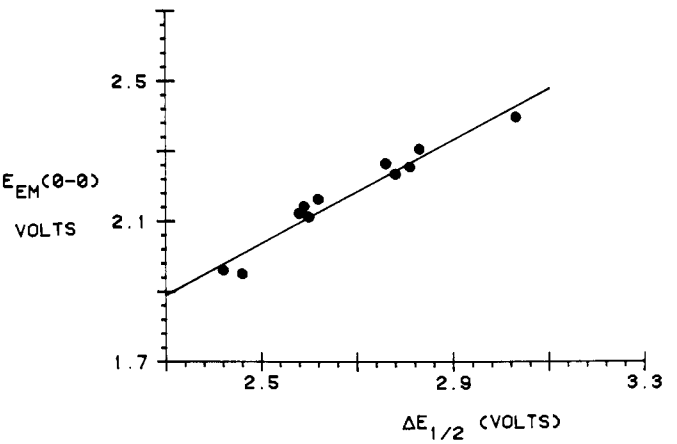

Figure 6. Plot of $\Delta E_{1/2}$ measured at room temperature in acetonitrile solution (0.1 M TEAP as supporting electrolyte) vs. $E_{em}(0\text{-}0)$ measured at 77 K in 4:1 ethanol/methanol glass for the series of $Ru(bpy)_2L_2^{2+}$ complexes. The least-squares line shown has slope 0.73 and intercept 0.21 eV. For the definitions of the variables, see the text.

calculations are also included in Table III.

Discussion

As outlined in the introduction, for the complexes $Ru(bpy)_2L_2^{2+}$ emission is generally observed from MLCT-based excited states that are largely triplet in character, but an additional complication exists as a result of the presence of a thermally accessible dd excited state or states. A goal of the present work was to discover the effect of nonchromophoric ligands on both MLCT decay and the transition between the MLCT and dd states. The approach taken here was systematic in that it was based on lifetime and emission quantum yield measurements on a series of related complexes of the type $Ru(bpy)_2L_2^{2+}$. The kinetic parameters of note for assessing the effects of ligand variations are the radiative and nonradiative decay rate constants (k_r and k_{nr}) and the temperature-dependent term characterizing the MLCT → dd transition, $k'^{\circ} \exp(-\Delta E'/RT)$. It should be noted that, although an extended series of compounds was investigated (Tables I and II), it was only possible to obtain a complete set of kinetics data for a limited number of compounds because of a loss in emission intensity at higher temperatures for several complexes. We will return to the probable origin of this effect below because it has important implications for the design of Ru(bpy) and related chromophores.

Excited-State Emission Energies and Reduction Potentials. It is known for complexes of the type $Ru(bpy)_2L_2^{2+}$ that the energy of the MLCT absorption band manifold increases in energy[22-24] linearly with increases in $\Delta E_{1/2}$, the difference in

(22) (a) Salmon, D. J. Ph.D. Dissertation, The University of North Carolina, Chapel Hill, NC, 1976. (b) Curtis, J. C.; Meyer, T. J. *Inorg. Chem.* **1982**, *21*, 1562.

reduction potentials for the metal-based Ru(III)/Ru(II) and ligand-based $bpy^{0/-}$ couples. A similar relationship for the emission process is shown in Figure 6 where the zero–zero emission energies ($E_{em}(0\text{–}0)$) for the series of complexes $Ru(bpy)_2L_2^{2+}$ are shown plotted vs. $\Delta E_{1/2}$. Absorption is dominated by intense transitions to MLCT states largely singlet in character,[2b] $Ru^{II}(bpy) \rightarrow Ru^{III}(bpy^{-}\cdot)$, and emission by transitions from states largely triplet in character,[4] $Ru^{III}(bpy^{-}\cdot) \rightarrow Ru^{II}(bpy)$, and the observation of such linear relationships strongly supports the assignment of the transitions. The observation of the linear relationship in Figure 6 for the entire series of complexes is also of value in demonstrating that, throughout the series, emission is occurring from states that have a common electronic origin.

It is revealing to inspect the redox potential data for the implications that it has for the origin of the variations in $\Delta E_{1/2}$ and consequently for the origins of variations in excited-state energies with variations in the ligands L. From the data in Table II, for complexes of the type $Ru^{II}(bpy)_2L_2^{2+}$ reduction potentials for the Ru(III)/Ru(II) couple vary over the range 0.94 to 1.75 V while the range for the ligand-based bpy reductions is much smaller, −1.28 to −1.48 V. The primary effect of variations in the ligand L is probably the relative stabilization of the Ru(II) state over Ru(III) by a combination of σ and π effects. The effect on the bpy reduction is small because the π^*(bpy) levels are removed from the direct site of Ru–L interaction and, as noted in earlier papers,[24] can therefore serve to act as "spectator ligands" for the Ru–L interaction.

From the arguments made above, variations in the MLCT excited-state energies are largely dictated by the Ru–L interaction. If it is assumed that the vibrational trapping energies associated with ground-state to excited-state structural variations are small, which they are for $Ru(bpy)_3^{2+}$, excited-state oxidation or reduction potentials can be calculated from eq 5 and 6, where $E^{\circ\prime}$ is the formal potential for the couple.[8] The values calculated for the excited-state couples are also shown in Table II.

$$E^{\circ\prime}(Ru(bpy)_2L_2^{3+/2+*}) \sim E^{\circ\prime}(Ru(bpy)_2L_2^{3+/2+}) - E_{em} \quad (5)$$

$$E^{\circ\prime}(Ru(bpy)_2L_2^{2+*/+}) \sim E^{\circ\prime}(Ru(bpy)_2L_2^{2+/+}) + E_{em} \quad (6)$$

With reference to Table II, the dominant feature in the excited-state redox potential variations is, once again, the Ru–L interaction. This observation has important consequences for the control of excited-state redox potentials by synthetic variations, a theme that will be developed in a later paper.

When the values of $E^{\circ\prime}(3+/2+^*)$ and $E^{\circ\prime}(2+^*/+)$ in Table II were calculated, $E_{em}(0\text{–}0)$ measured at 77 K in 4:1 ethanol/methanol glass was used for E_{em} and $E^{\circ\prime}(3+/2+)$ and $E^{\circ\prime}(2+/+)$ measured at 25 °C in CH_3CN solution was used. The use of two different media introduces a source of systematic error into the estimates of excited-state potentials. For $Ru(bpy)_3^{2+}$ the values are $E^{\circ\prime}(2+^*/+) = 0.77$ V and $E^{\circ\prime}(3+/2+^*) = -0.81$ V at 0.1 M ionic strength at 25 °C in CH_3CN solution,[8] compared to the values obtained here of 0.76 and −0.90 V. Consequently, the values reported here are probably valid at room temperatures in CH_3CN to within at least ±0.1 V. The difference in conditions for the two measurements was necessitated by the fact that several of the complexes of interest here do not emit appreciably at room temperature.

MLCT Excited-State Decay. MLCT excited-state lifetimes are determined by both radiative (k_r) and nonradiative (k_{nr}) processes. From Table III there is a variation in k_r (or as noted above in (k_r/ϕ_{isc})) through the series of only a factor of 1.9, if the anomalously low value for $Ru(bpy)_2py_2^{2+}$ is neglected.

The Einstein equation for spontaneous emission[20] is given in eq 7, where E is the energy of the emitted photon ($\sim E_{em}$-(0–0), the energy of the $v' = 0 \rightarrow v = 0$ emission (in cm^{-1}) as noted below) and the integral is the electronic transition moment between the excited (ψ_e) and ground (ψ_g) states between the $v'_M = 0$ and $v_M = 0$ levels. $\vec{d}$ is the transition moment operator. Using eq 7 and assuming that the transition moment stays constant give a predicted range in values for k_r of 1.5 for the excited states listed in Table III. The good agreement between the observed and calculated ranges for k_r and, by inference, the near constancy of the transition moments support the assumption of a common electronic origin for the series of emitting excited states. In addition, the relatively slight variations in k_r strongly support the suggestion that *variations* in ϕ_{isc} throughout the series cannot be too significant numerically.

$$k_r = \frac{4E^3}{3\hbar^4c^3}|\langle\psi_e|\vec{d}|\psi_g\rangle| \quad (7)$$

In principle, the electronic transition moment, μ, is obtainable from absorption spectra. However, the intensities of the direct optical transitions to the states responsible for emission are low, due to the largely singlet → triplet nature of the absorption.[4] In addition, they are obscured by the intense transitions to largely singlet MLCT states, which dominate the absorption spectra. The near constancy of μ throughout the series is not surprising if the emitting states have a common electronic origin. The magnitude of μ is determined by the metal and the chromophoric ligand, which remain common here, and by metal–ligand overlap.

Earlier work based on the MLCT excited states of the two series $Os^{II}(bpy)L_4^{2+}$ or $Os^{II}(phen)L_4^{2+}$ has shown that there is a firm theoretical basis for understanding rates of nonradiative decay processes based on the energy gap law for radiationless transitions.[6b,9,25] In the low-temperature ($\hbar\omega_M >> k_BT$) weak-vibrational-coupling ($(E_{em}(0\text{–}0)/\hbar\omega_M S_M) >> 1$) limit, the energy gap law can be written as[25,26]

$$\ln k_{nr} = \ln \beta_0 - S_M - \frac{\gamma_0 E_{em}(0\text{–}0)}{\hbar\omega_M} + \left(\frac{\chi_0}{\hbar\omega_M}\right)\left(\frac{k_BT}{\hbar\omega_M}\right)(\gamma_0 + 1)^2 \quad (8)$$

$$\beta_0 = (C^2\omega_k)\left(\frac{\pi}{2\hbar\omega_M(E_{em}(0\text{–}0) - \hbar\omega_k)}\right)^{1/2} \quad (9)$$

χ_0 is 4 times the classical solvent vibrational trapping or reorganizational energy associated with the transfer of the electron from the ligand to the metal. ω_M ($=2\pi\nu_M$) is the

(23) Lever, A. B. P.; Pickens, S. R.; Minor, P. C.; Licoccia, S.; Ramaswamy, B. S.; Magnell, K. *J. Am. Chem. Soc.* **1981**, *103*, 6800.
(24) Sullivan, B. P.; Baumann, J. A.; Meyer, T. J.; Salmon, D. J.; Lehmann, H.; Ludi, A. *J. Am. Chem. Soc.* **1977**, *99*, 7368.
(25) Caspar, J. V.; Kober, E. M.; Sullivan, B. P.; Meyer, T. J. *Chem. Phys. Lett.* **1982**, *91*, 91. Meyer, T. J. *Prog. Inorg. Chem.* **1983**, *30*, 389–440.
(26) (a) Freed, K. F.; Jortner, J. *J. Chem. Phys.* **1970**, *52*, 6272. (b) Lin, S. H. *Ibid.* **1966**, *44*, 3759. (c) Dixon, M.; Jortner, J. *Ibid.* **1968**, *48*, 715. (d) Englmann, R.; Jortner, J. *Mol. Phys.* **1970**, *18*, 145.
(27) Kober, E. M. Ph.D. Dissertation, The University of North Carolina, Chapel Hill, NC, 1982.
(28) Kober, E. M.; Caspar, J. V.; Sullivan, B. P.; Meyer, T. J., manuscript in preparation.
(29) (a) Marcus, R. A. *J. Chem. Phys.* **1956**, *24*, 979. (b) Dogonadze, R. R. In "Reactions of Molecules at Electrodes"; Hush, N. S., Ed.; Wiley-Interscience: New York, 1971. (c) Ulstrup, J. "Charge Transfer Processes in Condensed Media"; Springer-Verlag: New York, 1979. (d) Bottcher, C. J. F. "Theory of Electric Polarization"; Elsevier: New York, 1952; Chapter 5.
(30) (a) Caspar, J. V., unpublished results. (b) The relationship between $E_{em}(0\text{–}0)$ and E_{em} is of the form $E_{em}(0\text{–}0) = aE_m + b$ with $a \sim 1$ and b a negligible constant (~ 90 cm^{-1}).

angular frequency of the acceptor vibration or vibrations. ω_k ($=2\pi\nu_k$) is the angular frequency of the promoting vibration and C^2 the corresponding nuclear momentum matrix element. S_M ($=^1/_2\Delta_M^2$) is a measure of the extent of excited-state distortion in the acceptor vibration. Δ_M^2 is the dimensionless fractional displacement in the acceptor vibration between equilibrium geometries of the ground and excited states. In terms of a displacement coordinate Q (in cm), the dimensionless mass- and frequency-weighted coordinate q is given by $q = Q(M\omega/\hbar)^{1/2}$, where M is reduced mass of the vibration. The shift in equilibrium position of the ground state relative to the excited state for the mth normal vibration is given by $\Delta_M = q_e^e - q_e^g$, where q_e^e and q_e^g are the equilibrium normal coordinates for the excited and ground states. $E_{em}(0\text{–}0)$ is the emission energy for the $v'_M = 0 \rightarrow v_M = 0$ vibrational component. And γ_0 is defined as

$$\gamma_0 = \ln\left(\frac{E_{em}(0\text{–}0) - \hbar\omega_k}{\hbar\omega_M S_M}\right) - 1 \approx \ln\left(\frac{E_{em}(0\text{–}0)}{\hbar\omega_M S_M}\right) - 1 \tag{10}$$

Strictly speaking, eq 8 should also include contributions from the low-frequency metal–ligand modes for which evidence was obtained in the emission spectral fits. However, because of the low frequencies and small distortions involved, contributions to nonradiative decay involving these vibrations are negligible (<10%).[21c]

The successful application of eq 9 to explain observed trends in nonradiative decay rate constants in a series of related excited states requires that the following conditions be satisfied: (1) There must be a common acceptor vibration or vibrations. (2) The vibrationally induced electronic coupling between states that appears in the term $C^2\omega_k$ must remain relatively constant. (3) The solvent or vibrational trapping energy term, χ_0, must remain nearly constant. With regard to these three points in the context of the series $Ru(bpy)_2L_2^{2+}$, the following information is available: (1) The acceptor vibration(s) both in this work and in the earlier work on $(bpy)OsL_4^{2+}$ complexes appear to be ν(bpy) ring stretching in character.[3f,21c] This conclusion is based on the appearance of vibrational structure in the 77 K emission spectra (Table I) with spacings usually in the range 1300–1400 cm^{-1} and on the magnitudes of slopes of plots ln k_{nr} vs. E_{em} as discussed later. (2) The magnitude of C is determined by integrals of the form $\langle\psi_g|\partial/\partial Q_k|\psi_e\rangle$. In the integrals ψ_g and ψ_e are the ground- and excited-state electronic wave functions and Q_k is the coordinate of the promoting vibration or vibrations that, when activated, lead to changes in electronic overlap and thus to mixing between the two states.[26d,e] Given that the excited-state electronic structure involves an electron hole at the metal center and an unpaired electron in a ligand π^* orbital, vibrations that bring the electron–hole pair closer together would be expected to induce changes in ground- and excited-state overlap. This leads to the prediction that low-energy ($\sim$400 cm^{-1}) metal–ligand stretching and bending vibrations[31] should be the important promoting vibrations. Although the argument given here is qualitative, a more rigorous approach leads to identical conclusions.[27] For the series of Os^{II} complexes $(phen)Os^{II}L_4$, the available evidence clearly suggests that variations in the term $C^2\omega_k$ must be relatively small for a variety of ligands, L.[9,21c,28] (3) In the classical continuum limit the solvent vibrational trapping energy term χ_0 is given by eq 11,[29] where

$$\chi_0 = D\int(\vec{E}_f - \vec{E}_i)^2\,dV \tag{11}$$

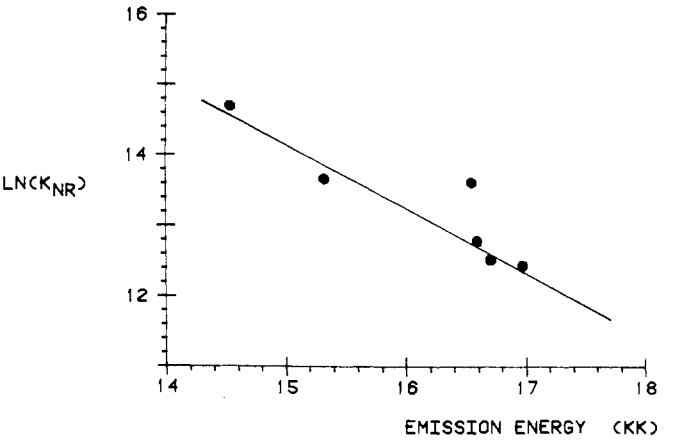

Figure 7. Plot of ln k_{nr} vs. E_{em}(200 K) for the series of complexes of the type *cis*-$Ru(bpy)_2L_2^{2+}$ (data from Table III).

D is a function of the optical and static dielectric constants of the solvent, $\vec{E}_i$ and $\vec{E}_f$ are the electric field vectors for the electronic distribution of the initial and final electronic states in a vacuum, and the integration is carried out over the volume surrounding the complex. The sense of the electron-transfer event, $(bpy^-\cdot)Ru^{III} \rightarrow (bpy)Ru^{II}$, is a feature in common for the series of excited-state decays. If k_{nr} values are obtained in a common solvent, χ_0 should be relatively constant. For the series of excited states studied here, variations in the term $(\chi_0/\hbar\omega_M)(k_BT/\hbar\omega_M)(\gamma_0 + 1)^2$, arising from the dependence of γ_0 on E_{em}, are expected to be less than 5%. Numerically this term is approximately equal to $\chi_0/\hbar\omega_M$ since $(k_BT/\hbar\omega_M)(\gamma_0 + 1)^2 \approx 1$ and for the complexes of interest here $\bar{\nu}_M \sim$ 1300–1400 cm^{-1} and $E_{em}(0\text{–}0) \sim$ 15000–17000 cm^{-1} (Table I).

Equation 8 is written in terms of the energy of the $v'_M = 0 \rightarrow v_M = 0$ transition, $E_{em}(0\text{–}0)$; however, the easily accessible experimental quantity at temperatures well above 77 K is the energy of the intensity maximum of the emission profile, E_{em}. Gaussian analyses of the 200 K emission spectra for the excited states of concern here show that the relationship $E_{em}(0\text{–}0) \sim E_{em}$ is valid.

From the comments above, eq 8 for ln k_{nr} can be rewritten as shown in eq 12. In order to reach the simplified form of eq 12, the approximation shown in eq 14 has been used, as well as the approximation that $(k_BT/\hbar\omega_M)(\gamma_0 + 1)^2 \sim 1$.

$$\ln k_{nr} = \ln\beta_0 - S_M + \left(\frac{\chi_0}{\hbar\omega_M}\right) - \frac{\gamma_0 E_{em}}{\hbar\omega_M} \tag{12}$$

$$\beta_0 = (C^2\omega_k)\left(\frac{\pi}{2\hbar\omega_M E_{em}}\right)^{1/2} \tag{13}$$

$$E_{em}(0\text{–}0) - \hbar\omega_k \sim E_{em}(0\text{–}0) \sim E_{em} \tag{14}$$

The terms ln β_0 and γ_0 are weakly varying functions of E_{em} so that eq 12 predicts that a plot of ln k_{nr} vs. E_{em} for a series of related excited states should be linear with a slope of $-\gamma_0/\hbar\omega_M$. As noted in the previous section, systematic variations in E_{em} in the series $Ru(bpy)_2L_2^{2+}$ occur because of variations in the interactions of the nonchromophoric ligand L and the metal center. In Figure 7 is shown a plot of ln k_{nr} vs. E_{em} (at 200 K) for the series $Ru(bpy)_2L_2^{2+}$, and the linearity of the plot is in obvious agreement with the prediction of eq 12.

The plot in Figure 7 uses values of E_{em} measured at 200 K rather than values at room temperature. The reason for this choice lies in the fact that in the fitting of the temperature-dependent lifetime data it was assumed that k_{nr} is temperature independent. In fact, emission spectra of all of the complexes investigated here show small but noticeable shifts to higher

(31) Nakamoto, N. "Infrared and Raman Spectra of Inorganic and Coordination Compounds", 3rd ed.; Wiley: New York, 1977; p 213.
(32) Young, R. C.; Meyer, T. J.; Whitten, D. G. *J. Am. Chem. Soc.* **1976**, *98*, 286.

Table IV. Values of the Slopes ($\partial \ln k_{nr}/\partial E_{em}$) and Intercepts ($E_{em} = 0$) from Plots of $\ln k_{nr}$ vs. E_{em} from Three Different Experimental Tests of the Energy Gap Law

source	slope, eV^{-1}	intercept, eV	ref
$Ru(bpy)_2L_2^{2+}$ compound series[a]	−7.49	28.05	this work
$Ru(bpy)_3^{2+}$ solvent dependence	−7.45	28.02	6b
$Os(bpy)L_4^{2+}$ compound series[b]	−7.54	29.17	9

[a] In CH_2Cl_2 solution. [b] In CH_3CN solution.

energy upon cooling to 200 K. Since eq 12 predicts that ln k_{nr} depends upon E_{em}, shifts in E_{em} with temperature lead to an apparent temperature dependence for k_{nr}. Such complications are avoided by using k_{nr} and E_{em} data obtained at the same temperature, and that, in a de facto way, is what is done in Figure 7. The E_{em} values were measured at 200 K, and at temperatures this low, k_{nr} is essentially independent of temperature, as shown, for example, by the data in Figure 5.

Because of the procedure adopted here, the values of the activation barriers for the transition to the dd state, $\Delta E'$, which are also obtained from the lifetime data, include a contribution from the temperature dependence of k_{nr} through E_{em}. For the Os–phen complexes mentioned above there are no complications from low-lying dd states and the temperature dependence of k_{nr} can be obtained directly. Those data show that at least for this type of MLCT excited state, the contribution of the temperature dependence of k_{nr} (through E_{em}) to $\Delta E'$ is probably relatively small ($\leq$400 cm^{-1}).[30a] However, the conclusion reached here need not always be true, and for systems exhibiting more dramatic temperature dependences of E_{em}, the effect may need to be considered explicitly in the interpretation of the data.

A more precise but experimentally far more tedious approach would have been to measure *all* of the parameters, τ_0, ϕ_r, and E_{em}, as a function of temperature. Using such a procedure would allow eq 12 to be tested at a series of temperatures and the temperature dependence of k_{nr} to be evaluated quantitatively.

A valuable comparison can now be made between the observed slopes and intercepts from plots of ln k_{nr} vs. E_{em} for three separate experiments: (1) $Ru(bpy)_2L_2^{2+}$ and (2) $Os(bpy)L_4^{2+}$, where variations in E_{em} are also induced by changes in the ligand L,[9] and (3) $Ru(bpy)_3^{2+}$, where variations in E_{em} were induced by variations in solvent.[6b] (Comparisons using $Ru(bpy)_3^{2+}$ based on solvent variations do not include results for hydroxylic solvents like water and methanol, where strong, specific solvent effects appear to exist.[6b,25])

From the three different sets of data a number of significant conclusions can be drawn:

(1) According to eq 12, if the acceptor vibration or vibrations remain the same, plots of ln k_{nr} vs. E_{em} should be a series of three parallel lines having the same slope. That they are is shown by the slopes and intercepts obtained from the plots for the three experiments, as summarized in Table IV.

(2) Given the terms that appear in the intercept in eq 13, it is significant that the intercepts for the $Ru(bpy)_2L_2^{2+}$ experiment and the $Ru(bpy)_3^{2+}$ solvent-dependence experiment are identical within experimental error. The observation suggests that the magnitude of C^2, which is contained within the term ln β_0, is determined largely by the electronic structure of the chromophoric ligand if the metal is held constant.

(3) It is also of significance that the intercept for the Os data is higher than for the Ru data. If it is assumed that the frequency of the promoting vibration is the same for both cases, which seems reasonable, given that the metal–nitrogen bending and stretching frequencies are expected to be nearly the same,[31] the difference in intercepts between Ru and Os must occur largely in C^2, and from eq 13 and the data in Table IV, $C_{Os}^2 \sim 3C_{Ru}^2$. This is not a surprising result since C involves electronic overlap type terms:

$$C^2 = \frac{\hbar^2}{M_k}\left|\left\langle \psi_g \left| i\frac{\partial}{\partial Q_k} \right| \psi_e \right\rangle\right|^2$$

where M_k is the reduced mass of the promoting vibration and the operator $\partial/\partial Q_k$ is not a function of spin. The ground state is largely singlet in character because the lowest lying triplet states are relatively high in energy, $E_{em} \sim 2$ V. As a consequence, the magnitude of C^2 will increase linearly with the extent of singlet character in the nominally triplet excited states. The triplet excited states have appreciable singlet character because of mixing with low-lying singlet excited states induced by spin–orbit coupling.[2b,4] When written as a linear combination of singlet ($^1\psi_e$) and triplet ($^3\psi_e$) components, the excited-state wave function is $\psi_e = \alpha_1(^1\psi_e) + \alpha_3(^3\psi_e)$. Calculations based on a parameterized spin–orbit coupling model for the dominant emitting excited states of $Ru(bpy)_3^{2+}$ and $Os(bpy)_3^{2+}$ predict that, while $(\alpha_3)^2 = 0.10$–0.15 for $Os(bpy)_3^{2+}$, it is lower by a factor of $\sim$3 for $Ru(bpy)_3^{2+}$.[27] The decrease in singlet character for Ru follows from a decrease in spin–orbit coupling, as shown by its decreased spin–orbit coupling constant, $\lambda_{Os} \sim 3\lambda_{Ru}$. The calculated ratio of $(\alpha_3(Os))^2/(\alpha_3(Ru))^2 \sim 3$ is near the experimental ratio of $C^2_{Os}/C^2_{Ru} = 3$. Consequently, it appears reasonable to suggest that perhaps the primary origin of the difference in C^2 between Ru and Os is the enhanced singlet character of the Os excited states resulting from the larger magnitude of the spin–orbit coupling constant for Os compared to that of Ru. The net effect of the increase in C_{Os} compared to C_{Ru} is to increase k_{nr} by a factor of 3 for complexes of Os(II) compared to complexes of Ru(II) that *have the same emission energy.*

The fact that the compound $Ru(bpy)_2(phen)^{2+}$ lies on the line of the plot of ln k_{nr} vs. E_{em} in Figure 7 is worth some discussion. In our previous studies on Os–bpy and Os–phen complexes,[9] we observed that plots of ln k_{nr} vs. E_{em} were linear, with the two groups of compounds having parallel slopes but substantially different intercepts. If it is assumed that ω_k is the same for the Os–bpy and Os–phen complexes, the increase in intercept for the bpy complexes suggests that $C^2(bpy) \sim 3C^2(phen)$. That a similar relationship exists for Ru–bpy and Ru–phen complexes can be shown on the basis of the data for $Ru(phen)_3^{2+}$ in Table III and the plot of ln k_{nr} vs. E_{em} for Ru–bpy complexes in Figure 7. From the experimental dependence of ln k_{nr} on E_{em} in Figure 7, a Ru–bpy complex having the same value of E_{em} at 200 K in methylene chloride solution as does $Ru(phen)_3^{2+}$ ($E_{em} = 17.12 \times 10^3$ cm^{-1}) would have $k_{nr} = 1.9 \times 10^5$ s^{-1}. In fact, $k_{nr} = 6.7 \times 10^4$ s^{-1} for $Ru(phen)_3^{2+}$, which is slower by a factor of 2.8. The fact that k_{nr} for $Ru(bpy)_2(phen)^{2+}$ falls near the line in Figure 7 shows that nonradiative decay is dominated by the bpy ligands. If the excited electron were localized but equally distributed over the three ligands, decay from bpy-based MLCT states would be expected to dominate because of the statistical factor of 2 and the larger k_{nr} value associated with bpy as the acceptor ligand. In addition, for the mixed-chelate complex, a single exponential decay is observed over the temperature range 225 K–room temperature. The latter result suggest that electron transfer among the ligands must be rapid on the time scale for excited-state decay. This conclusion is consistent with the reported intramolecular bpy/(bpy$^-$·) self-exchange rate constant (k_{ex}) for $[(bpy^-\cdot)Fe(bpy)_2]^+$, $k_{ex}(297\ K) = 2 \times 10^8$ s^{-1},[33] which is larger than k_{nr} for $[Ru(bpy)_2(phen)]^{2+}$ by a factor of 700. Since the ligand to ligand self-exchange rate constant should be dictated primarily by solvent and by ligand-localized,

(33) Motten, A. G.; Hanck, K.; DeArmond, M. K. *Chem. Phys. Lett.* **1981**, *79*, 541.

intramolecular vibrational trapping, k_{ex} should be similar for $[(bpy^{-}\cdot)Fe(bpy)_2]^+$ and $[(bpy^{-}\cdot)Ru(bpy)_2]^+$ and should be comparable for the excited states $[(bpy^{-}\cdot)Ru^{III}(bpy)_2]^{2+*}$ and $[(bpy^{-}\cdot)Ru^{III}(phen)(bpy)]^{2+*}$ as well.

The MLCT → dd Transition. From earlier work on $Ru(bpy)_3^{2+}$,[6,7] $Ru(phen)_3^{2+}$,[6] and $Ru(bpy)_2(py)_2^{2+}$,[6a,16] the origin of the temperature-dependent term in the lifetime expression in eq 1 can most readily be explained as a thermally activated transition from the MLCT state to a low-lying, Ru-based dd state. Once populated, the dd state appears to undergo either photochemistry or rapid decay to the ground state. For $Ru(bpy)_2(py)_2^{2+}$ in CH_2Cl_2, photosubstitution of py by anions is highly efficient with $\phi_p \sim 0.3$,[16] while for $[Ru(bpy)_3](Cl)_2$ at 25 °C, formation of $Ru(bpy)_2Cl_2$ occurs with $\phi_p = 0.10$.[6a]

Having available the series of complexes $Ru(bpy)_2L_2^{2+}$ gave us the opportunity to explore the effects of variations in nonchromophoric ligands on the MLCT → dd transition. Values of k° and $\Delta E'$ for the complexes are given in Table III. It is clear from the data that changes in L lead to experimentally significant variations in the two parameters with k° ranging from 1.7×10^{13} to 8.8×10^{13} s^{-1} and $\Delta E'$ from 2560 to 3560 cm^{-1}. From a kinetic analysis of the dynamics of the MLCT → dd transition based on the sequence of reactions in Scheme II, the experimentally observed rate constant, $k' = k^{\circ} \exp(-\Delta E'/kT)$, can be written in terms of the rate constants in the scheme as shown in eq 15. In the limit

Scheme II

$$\text{MLCT} \underset{k_{-2}}{\overset{k_2}{\rightleftharpoons}} \text{dd}$$

$$\text{dd} \xrightarrow[k_3]{} \text{photochemistry or decay}$$

$$k' = k_2\left(\frac{k_3}{k_{-2} + k_3}\right) \tag{15}$$

that $k_{-2} >> k_3$, the dd state is in equilibrium with the MLCT state and k' is related to k_2, k_{-2}, and k_3 as shown in eq 16. In the other limit ($k_3 >> k_{-2}$), k' is given by eq 17.

$$k' = \left(\frac{k_2}{k_{-2}}\right)k_3 \tag{16}$$

$$k' = k_2 = A \exp(-E_a/kT) \tag{17}$$

Recent work with bpy–bipyridimidine and bpy–bipyrazine mixed chelates of Ru(II) suggests that compounds exist which correspond to both limiting cases. Examples of the first limiting case ($k_{-2} >> k_3$) are characterized by values of both $\Delta E'$ ($\sim$2000 cm^{-1}) and k° ($\sim 10^9$ s^{-1}), which are relatively small. For the second case both kinetic parameters are larger ($\Delta E'$ $\sim$ 2500–4000 cm^{-1}; $k^{\circ} \sim 10^{12}$–10^{14} s^{-1}).[34] For the Os^{II}–bpy or –phen complexes, where $10Dq$ is $\sim$30% larger than for the Ru^{II} complexes, dd states appear to be thermally inaccessible, at least near ambient temperatures, and excited-state lifetimes are nearly temperature independent at temperatures in excess of 200 K.

Returning to the data in Table III, it appears that, for the MLCT → dd surface crossing, all of the compounds described here fall into the second case, where irreversible surface crossing occurs and $k' = k_2$. In this limit, the parameters $\Delta E'$ and k° become simply the energy of activation, E_a(dd), and the preexponential term, $k^{\circ} = k^{\circ}_2 = A$, for the MLCT → dd surface crossing. The surface crossing is an excited-state internal conversion process, but it can also be viewed as an intramolecular electron-transfer reaction, $d\pi^5\pi^* \rightarrow d\pi^5 d\sigma^*$, where the electron transfer is from π^*(bpy) to $d\sigma^*$(Ru).

In an earlier study on the solvent dependence of the photophysical properties of $Ru(bpy)_3^{2+*}$, it was possible to account qualitatively for the observed trends in the data for k°_2 and E_a(dd) by assuming that the major effect of solvent variations was in the stabilization or destabilization of the MLCT excited state relative to the nearly solvent-independent dd state.[6b] Examination of the data for $Ru(bpy)_2L_2^{2+}$ in Table III shows that, in contrast to the results of the solvent-dependence study, there does not appear to be any systematic trend in the values of k° and $\Delta E'$ that can be related to specific properties of the ligands L. This is hardly a surprise. From electron-transfer theory, E_a(dd) is expected to be strongly dependent on the relative energies of the MLCT and dd states.[6b] Although a reasonably clear, if qualitative, pattern is available to explain how the energy of the MLCT state varies with L, at present we do not have a useful model for predicting how the energy of the dd states varies with L.

Excited-State Properties of Related Complexes. For the complexes of the type $Ru(bpy)_2L_2^{2+}$ where L is a phosphine or arsine ligand, *cis*-$[Ru(bpy)_2(PR_3)_2]^{2+}$ or *cis*-$[Ru(bpy)_2(AsR_3)_2]^{2+}$, an appreciable emission can only be observed at very low temperatures ($T \leq 150$ K). A measurable luminescence is virtually undetectable above 200 K in CH_2Cl_2. Given the earlier work on $Ru(bpy)_3^{2+}$ and the results obtained here, this seeming anomaly can be explained in a reasonable and systematic fashion.

The phosphine and arsine complexes are all high-energy emitters at 77 K in alcohol glasses ($E_{em}(0\text{–}0)$ = (17.95–19.30) $\times 10^3$ cm^{-1}, consistent with the back-bonding abilities of the ligands and the observed values of $\Delta E_{1/2}$ at room temperature; note the data in Figure 6. That the emissions for the phosphine and arsine complexes remain MLCT in nature is shown by the fact that their emission energies fall on the plot of E_{em} vs. $\Delta E_{1/2}$ in Figure 6. It can also be predicted that the MLCT excited states are intrinsically long-lived. From the plot of ln k_{nr} vs. E_{em} in Figure 7 and the emission energies in Table III, values of k_{nr} in the range of 2×10^4 to 9×10^4 s^{-1} should exist for the MLCT excited states of the complexes. Because of the magnitudes of the energy gaps involved, the MLCT states should be inherently long-lived and they should be efficient emitters. For example, on the basis of $k_r = 10^5$ s^{-1} and the values of k_{nr} mentioned above, ϕ_r should be in the range 0.5–0.8 and τ_0 should be in the range of 5–8 μs.

The phosphine and arsine complexes have the expected excited-state properties but only at low temperatures. Although values of ϕ_r have not been measured, the complexes are extremely intense emitters, and for $[Ru(bpy)_2(Me_2P(CH_2)_2PMe_2)]^{2+}$ in a 4:1 EtOH/MeOH glass at 77 K, τ_0 = 6.2 μs. Furthermore, for excited states of complexes of the type $Os(bpy)L_4^{2+}$ and $Os(phen)L_4^{2+}$ that contain phosphine or arsine ligands, no unusual deactivation pathways have been encountered either at room temperature or at 77 K.[9] A reasonable and self-consistent explanation for the shortened lifetimes and inefficient emission yields at higher temperatures for the Ru complexes is in an enhanced rate for the MLCT → dd transition compared, for example, to that of $Ru(bpy)_3^{2+}$, where k'(298 K) = 1.7×10^6 s^{-1}.

To put the situation into perspective numerically, assuming first that the rate equation for k_2 has the form $k' = k_2 = 10^{13} \exp(-E_a/RT)$, second that ϕ_r ($=k_r/(k_r + k_{nr} + k')$) is $\sim 10^{-6}$ at room temperature, which is at the limit of our detection capabilities, and third that $k_r = 1 \times 10^5$ s^{-1}, we estimate that an *upper* limit for E_a(dd) is $\sim$850 cm^{-1} ($k_2 = 1.7 \times 10^{11}$ s^{-1} at 298 K) for the phosphine and arsine complexes. Apparently, the effect of the phosphine or arsine ligands compared to that

(34) Rillema, D. P.; Allen, G. H.; Meyer, T. J., submitted for publication.
(35) Figgis, B. N. "Introduction to Ligand Fields"; Interscience: New York, 1966.

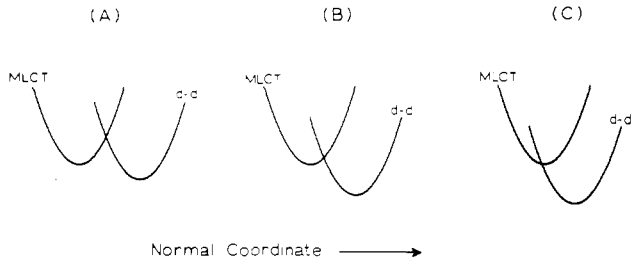

Figure 8. Schematic illustration of the effects of ligand variations on the relative energies of the dd and MLCT excited states for the complexes *cis*-$Ru(bpy)_2LL'^{2+}$: (A) L = nitrogen-donor ligand ($\Delta E'$ = 2700–3600 cm^{-1}); (B) L = tertiary phosphine or arsine ($\Delta E' < 850$ cm^{-1}); (C) L = CO, L' = Cl^- ($\Delta E' < 150$ cm^{-1}). The drawing is not to scale.

of a third bpy is to destabilize the MLCT state to a far greater extent than the dd state. The net effect is to decrease the thermal activation required to reach the intersection region, thus greatly enhancing the MLCT → dd transition rate.

An extreme case of the effect discussed above is probably exhibited by the complex *cis*-$[Ru(bpy)_2(CO)Cl]^+$. If the $\Delta E_{1/2}$ value in Table II and the correlation between electrochemical and emission data in Figure 6 are used, the complex is predicted to have $E_{em}(0\text{–}0) \sim 18 \times 10^3$ cm^{-1} at 77 K in 4:1 EtOH/MeOH glass. In the absence of a low-lying dd state the complex should have $k_{nr} = 8 \times 10^4$ s^{-1} and $\phi_r \sim 0.5$. In fact, there is no detectable emission from *cis*-$[Ru(bpy)_2(CO)Cl]^+$ at this energy even at 77 K. If the same calculational procedure mentioned above is followed for the phosphine complexes, an *upper limit* of the thermal barrier to MLCT → dd electron transfer is ~150 cm^{-1} for $[Ru(bpy)_2(CO)Cl]^+$. It is entirely likely that for the carbonyl complex not only is the dd state the lowest excited state but the MLCT state is nested inside the dd potential curve, as shown in Figure 8. A lowest lying, efficiently populated dd state would be consistent with the reported observation that $[Ru(bpy)_2(CO)Cl]^+$ is extremely photoactive at room temperature with loss of CO as the major photopathway.[15b] It is interesting to note that an analogous situation exists for the excited states of $Fe(bpy)_3^{2+}$, where it has been shown that the initially formed MLCT state is rapidly (τ = 0.6 ns) converted into a lower lying dd state.[3a]

Implications for Excited-State Properties and Catalyst Design. The results obtained here have some important implications for the photophysical and photochemical properties of MLCT excited states and for their use in the design of potential photocatalysts: (1) The variations in k_r and k_{nr} induced by changes in the nonchromophoric ligands can be understood by using available theory. Of special importance is the success of radiationless decay theory in accounting for k_{nr}. (2) The existence of linear correlations between ln k_{nr} and E_{em} and between $\Delta E_{1/2}$ and E_{em} are noteworthy. It is true that for Ru and Os bpy- or phen-based MLCT excited states a *simple electrochemical measurement is sufficient to establish with reasonable accuracy E_{em}, k_{nr}, and excited-state redox potentials.* (3) MLCT excited-state lifetimes can be increased by designing complexes having large energy gaps between ligand- and metal-based redox levels. However, increasing the energy gap can be a self-defeating proposition for two reasons. The first is a significant decrease in visible light absorption as MLCT band maxima shift into the UV. The second is that, as the energy increases, k_{nr} *decreases* but k_r *increases*, if at a slower rate. In the limit, k_r will dictate excited-state lifetimes at least for the Os complexes where there is no complication from decay through a dd channel. (4) With an even higher MLCT energy gap induced by variations in ligands, the MLCT state could be sufficiently destabilized that other states could be lowest lying. The most notable possibilities are ligand-localized $\pi\pi^*$ states that have been observed in systems containing Rh^{III} and Ir^{III}.[11b,36] (5) The intervention of low-lying dd states for the Ru complexes is a major problem. At best, the presence of the dd state represents a nuisance decay pathway—~98% of excited-state decay for $Ru(phen)_3^{2+}$ in CH_2Cl_2 at room temperature occurs through the dd state.[6a] At worst, dd states represent major sources of photoinstability, e.g., $Ru(bpy)_2(py)_2^{2+*}$, where ϕ for loss of py is ~30%, or severely limit excited-state lifetimes, e.g., $Ru(bpy)_2(PR_3)_2^{2+*}$. In part, the photoinstability of complexes like $Ru(bpy)_3^{2+}$ is somewhat lessened because of intramolecular chelate ring closure in intermediates like $[(bpy)_2Ru(H_2O)(bpy)]^{2+}$. There is no such "self-annealing" effect for unidentate complexes of the type $Ru(bpy)_2L_2^{2+}$ where the expelled ligand is lost into the medium. Further work is needed to establish ligand effects on the energy difference between the MLCT and dd states before the dd states can be "designed out" of the complexes; however note ref 34. (5) As noted above, one approach to avoiding the intervention of dd states is to turn to Os, where $10Dq$ is sufficient to ensure a large gap between the MLCT and dd states. However, initial experiments suggest that even here, if the symmetry is lowered, e.g., by using 2,2′,2″-terpyridine as the chromophoric ligand, or the MLCT state is raised sufficiently above the ground state by ligand variations, photosubstitutional pathways begin to appear.[37] As a corollary, the notable absence of long-lived MLCT excited states based on iron is hardly surprising, given the much smaller value of $10Dq$ and the existence of lower lying dd states.

Acknowledgment is made to the National Science Foundation under Grant No. CHE-8008922 for support of this research and to Dr. H. Yerzin for sending us a preprint of his work on polarized emission from $Ru(bpy)_3^{2+}$.

Registry No. $Ru(bpy)_2(AEP)^{2+}$, 56889-69-1; $Ru(bpy)_2(NMI)_2^{2+}$, 85719-79-5; $Ru(bpy)_2(py)_2^{2+}$, 63338-38-5; $Ru(bpy)_3^{2+}$, 15158-62-0; $Ru(bpy)_2(phen)^{2+}$, 22563-13-9; $Ru(bpy)_2(pyd)_2^{2+}$, 85719-80-8; $Ru(bpy)_2(CO)Cl^{2+}$, 85719-81-9; $Ru(bpy)_2(dmpe)^{2+}$, 85719-82-0; $Ru(bpy)_2(diars)^{2+}$, 85719-83-1; *trans*-$Ru(bpy)_2(PPh_2Me)_2^{2+}$, 85761-22-4; *cis*-$Ru(bpy)_2(PPh_2Me)_2^{2+}$, 67674-01-5; $Ru(bpy)_2(dppene)^{2+}$, 67673-97-6; $Ru(phen)_3^{2+}$, 22873-66-1.

Supplementary Material Available: Tables of emission lifetimes in methylene chloride solution as a function of temperature (7 pages). Ordering information is given on any current masthead page.

(36) Watts, R. J.; Griffith, B. G.; Harrington, J. S. *J. Am. Chem. Soc.* **1976**, *98*, 674.
(37) Allen, G.; Sullivan, B. P.; Meyer, T. J. *J. Chem. Soc., Chem. Commun.* **1981**, 793.